Since January 2020 Elsevier has created a COVID-19 resource centre with free information in English and Mandarin on the novel coronavirus COVID-19. The COVID-19 resource centre is hosted on Elsevier Connect, the company's public news and information website.

Mechanisms of Ageing and Development 202 (2022) 111636

Contents lists available at ScienceDirect

Mechanisms of Ageing and Development

journal homepage: www.elsevier.com/locate/mechagedev

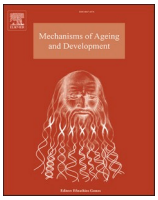

Circulating miR-320b and miR-483-5p levels are associated with COVID-19 in-hospital mortality☆

Angelica Giuliani [a,1], Giulia Matacchione [a,1], Deborah Ramini [b,1], Mirko Di Rosa [b,1], Anna Rita Bonfigli [c], Jacopo Sabbatinelli [a,d,*], Vladia Monsurrò [e], Rina Recchioni [b], Fiorella Marcheselli [b], Francesca Marchegiani [b], Francesco Piacenza [f], Maurizio Cardelli [f], Roberta Galeazzi [g], Giovanni Pomponio [h], Alessia Ferrarini [h], Armando Gabrielli [a,h], Silvia Svegliati Baroni [a], Marco Moretti [d], Riccardo Sarzani [a,i], Piero Giordano [i], Antonio Cherubini [j], Andrea Corsonello [k,l], Roberto Antonicelli [m], Antonio Domenico Procopio [a,g], Manuela Ferracin [n], Massimiliano Bonafè [n], Fabrizia Lattanzio [c], Fabiola Olivieri [a,b]

[a] Department of Clinical and Molecular Sciences, Università Politecnica delle Marche, Ancona, Italy
[b] Center of Clinical Pathology and Innovative Therapy, IRCCS INRCA, Ancona, Italy
[c] Scientific Direction and Geriatric Unit, IRCCS INRCA, Ancona, Italy
[d] SOD Medicina di Laboratorio, Azienda Ospedaliero Universitaria Ospedali Riuniti, Ancona, Italy
[e] Department of Medicine, University of Verona, Verona, Italy
[f] Advanced Technology Center for Aging Research, Scientific Technological Area, IRCCS INRCA, Ancona, Italy
[g] Clinical Laboratory and Molecular Diagnostic, Italian National Research Center on Aging, IRCCS INRCA, Ancona, Italy
[h] Clinica Medica, Department of Internal Medicine, Ospedali Riuniti, Ancona, Italy
[i] Internal Medicine and Geriatrics, Italian National Research Centre on Aging, Hospital "U. Sestilli", IRCCS INRCA, via della Montagnola n. 81, 60127, Ancona, Italy
[j] Geriatria, Accettazione geriatrica e Centro di Ricerca Per l'invecchiamento, IRCCS INRCA, Ancona, Italy
[k] Geriatric Medicine, IRCCS INRCA, 87100 Cosenza, Italy
[l] Unit of Geriatric Pharmacoepidemiology and Biostatistics, IRCCS INRCA, 87100 Cosenza, Italy
[m] Cardiology Unit, IRCCS INRCA, 60129 Ancona, Italy
[n] Department of Experimental, Diagnostic, and Specialty Medicine (DIMES), University of Bologna, Bologna, Italy

ARTICLE INFO

Keywords:
COVID-19
MicroRNA
In-hospital mortality
MiR-320b
MiR-483-5p

ABSTRACT

The stratification of mortality risk in COVID-19 patients remains extremely challenging for physicians, especially in older patients. Innovative minimally invasive molecular biomarkers are needed to improve the prediction of mortality risk and better customize patient management. In this study, aimed at identifying circulating miRNAs associated with the risk of COVID-19 in-hospital mortality, we analyzed serum samples of 12 COVID-19 patients by small RNA-seq and validated the findings in an independent cohort of 116 COVID-19 patients by qRT-PCR. Thirty-four significantly deregulated miRNAs, 25 downregulated and 9 upregulated in deceased COVID-19 patients compared to survivors, were identified in the discovery cohort. Based on the highest fold-changes and on the highest expression levels, 5 of these 34 miRNAs were selected for the analysis in the validation cohort. MiR-320b and miR-483-5p were confirmed to be significantly hyper-expressed in deceased patients compared to survived ones. Kaplan-Meier and Cox regression models, adjusted for relevant confounders, confirmed that patients with the 20% highest miR-320b and miR-483-5p serum levels had three-fold increased risk to die during in-hospital stay for COVID-19. In conclusion, high levels of circulating miR-320b and miR-483-5p can be useful as minimally invasive biomarkers to stratify older COVID-19 patients with an increased risk of in-hospital mortality.

☆ Trial registration number: NCT04348396, Registration date 16 Apr 2020.

* Correspondence to: Department of Clinical and Molecular Sciences, Università Politecnica delle Marche, Ancona, Italy.
E-mail address: j.sabbatinelli@pm.univpm.it (J. Sabbatinelli).

[1] Contributed equally to the manuscript.

https://doi.org/10.1016/j.mad.2022.111636
Received 30 November 2021; Received in revised form 13 January 2022; Accepted 31 January 2022
Available online 2 February 2022

1. Introduction

The ongoing severe acute respiratory syndrome, named coronavirus disease 2019 (COVID-19) and caused by severe acute respiratory syndrome (SARS) related coronavirus 2 (SARS-CoV-2) has become one of the greatest threats to our health and to social/economic stability worldwide (Zhou et al., 2020). The course of the disease shows wide variability, ranging from completely asymptomatic presentations to disease associated with severe clinical outcomes. Nowadays, COVID-19 is recognized as the primary cause of mortality in humans (Elezkurtaj et al., 2021). Older adults and people who have severe underlying medical conditions, like heart and lung diseases, diabetes, or immune and inflammatory chronic conditions, have the highest risk of developing serious complications from COVID-19 (Bonafè et al., 2020; Wu et al., 2020). The elderly population is the most susceptible to an uncontrolled inflammatory response induced by SARS-CoV-2 infection, named cytokine storm, that most likely plays important roles in platelet activation, coagulopathy, and venous thromboembolism (Ahmad et al., 2021; Liu et al., 2021). Cytokine storm is characterized by increased levels of several proinflammatory cytokines, such as IL-6, IL-1β, and TNF-α, and it is an important factor leading to the death of patients affected by COVID-19 (Jia et al., 2021; Mehta et al., 2020; Ruan et al., 2020). The pharmacological blockade of IL-6 has become the pivotal focus of the therapeutic strategies since the very beginning of the COVID-19 pandemic (reviewed in Campochiaro et al., 2021). In the most recent prospective meta-analysis of clinical trials of patients hospitalized for COVID-19, administration of IL-6 antagonists, compared with usual care or placebo, was associated with lower all-cause mortality, without a higher number of serious adverse events, thus confirming that IL-6 is a functional biomarker of COVID-19 severity (Group et al., 2021; Lo and Chagla, 2021; Vela et al., 2021). However, increasing evidence suggested that therapeutic interventions to reduce IL-6 are effective when the baseline mortality risk is high, while they could be harmful when the baseline mortality risk is low (Malgie et al., 2021). Overall, not all patients might equally benefit from immunosuppressive treatments, with probably a greater potential benefit for patients with significantly greater systemic inflammation (Cavalli et al., 2021; Della-Torre et al., 2021).

Therefore, to reduce COVID-19 severe outcomes, innovative molecular biomarkers are needed to improve the stratification of patients at the highest risk of mortality and to better customize therapeutic strategies.

The demonstration that circulating RNAs (especially microRNAs) constitute a new system for inter-tissue and inter-organ communication besides the classic mechanisms (hormones, cytokines, growth factors) has been a revolutionary biomedical discovery, intensively investigated in recent years (Chen et al., 2021). This communication system provides an additional level of control of cell homeostasis, safeguarding the functional state of biological systems and thus affecting the likelihood of developing several human diseases (Olivieri et al., 2021). MicroRNAs associated with COVID-19 outcomes could allow quantifying the risk of severe outcomes and developing models for predicting outcomes, thus helping to customize the most aggressive therapeutic strategies for each patient. Few recent studies investigated circulating microRNAs potentially associated with COVID-19 severity and mortality (de Gonzalo-Calvo et al., 2021; Gutmann et al., 2021; Parray et al., 2021).

Recently, we demonstrated that serum levels of microRNAs involved in the modulation of inflammation (Olivieri et al., 2021, 2013), were associated with the clinical response to anti-IL-6 receptor therapy in a sample of COVID-19 patients (Pomponio et al., 2021; Sabbatinelli et al., 2021).

In this study, we analyzed the circulating miRNA profile in two independent cohorts of COVID-19 patients, that is, a discovery and a validation cohort, with the aim to identify miRNAs associated with COVID-19 in-hospital mortality.

2. Patients and methods

2.1. Study design and participants

The present study is designed as a 2-phase study, including a discovery and a validation cohort to identify circulating serum miRNAs associated with in-hospital mortality for COVID-19.

In the discovery phase, all the expressed miRNAs were analyzed through small RNA-seq in serum samples of 12 COVID-19 patients, 6 alive and 6 deceased during the in-hospital stay at Ospedali Riuniti, Ancona, Italy. MiRNAs significantly different among alive and deceased patients identified in the discovery cohort were validated through qRT-PCR in an independent cohort of 116 COVID-19 patients, 75 alive and 41 deceased during the in-hospital stay at INRCA hospital, Ancona, Italy.

2.2. COVID-19 patients enrolled for the discovery phase

Twelve biological samples were selected from the COVID-19 patients enrolled at baseline in the framework of a Phase-2 clinical trial evaluating the anti-IL-6 drug Tocilizumab for the treatment of COVID-19 pneumonia (Pomponio et al., 2021). Twelve samples were chosen among 46 patients enrolled up to 31st May 2020 based on their outcome – 6 survived and 6 deceased during the in-hospital stay – and on the availability of baseline serum samples (Table 1a). None of these patients had received anti-COVID-19 vaccine. Both serum samples, collected at the time of hospital admission, and clinical data were available for this set of patients. Only serum samples at baseline, before treatment, were selected for the discovery phase. Small RNA-seq profiling was performed on the 12 selected serum samples.

2.3. COVID-19 patients enrolled for the validation phase

116 serum samples and clinical data were selected from the Report-Age COVID-19 database, an observational study conducted at the Italian National Center on Aging (IRCCS INRCA) aimed at deepening the understanding of COVID-19 in older patients hospitalized and diagnosed with COVID-19. The 116 patients were selected from the database, based on the availability of serum samples collected at the time of hospital admission and clinical data. All the patients enrolled in the Report-Age COVID-19 study had been confirmed to have COVID-19 and received treatment from INRCA hospital from 1st March 2020–24 th June 2021. Among these patients, we selected 116 patients consecutively admitted to INRCA Hospital between 11th October and 31st December 2020 for the validation cohort. None of these patients had received the anti-COVID-19 vaccine. The confirmed case was defined as a patient who had been confirmed to be infected by SARS-CoV-2 by real-time reverse transcriptase-polymerase chain reaction assay regardless of the clinical symptoms. The most frequent comorbidities were reported in Table 1b.

With respect to medications, most of the patients received corticosteroids during their hospital stays with no significant difference between deceased and survived. None of these patients received Tocilizumab as a treatment for COVID-19.

2.4. Ethics statement

The patients selected for the discovery phase were enrolled in the framework of a previously described clinical trial (NCT04315480) (Pomponio et al., 2021). Patients selected for the validation phase were enrolled according to The Report-Age protocol study that has been approved by the Ethics Committee of the IRCCS INRCA, Ancona, Italy (reference number CE-INRCA-20008) and registered under the ClinicalTrials.gov database (reference number NCT04348396). All the statistical analysis was done on anonymized data. All research was conducted in accordance with relevant guidelines and regulations.

2.5. Data collection

Clinical and epidemiological data were collected in a retrospective manner and were anonymized before release. Demographic data including age, sex, and survival status were collected. The categories of comorbidities were assessed including diabetes mellitus, hypertension, heart failure, chronic heart disease, asthma, chronic obstructive pulmonary disease, chronic kidney disease, malignancy, chronic liver disease, connective tissue disease, and dementia. The Charlson Comorbidity Index (CCIS) was calculated as previously described (Charlson et al., 1987).

Clinical Frailty Scale (CFS), a 9-point scale ranging from 1 (very fit) to 9 (severely frail), was used to assess frailty (Rockwood et al., 2005). Patients were divided into three groups based on their frailty scores. Patients who were scored at 1–3 on the CFS were defined as not frail (group 1), patients who were scored at 4–7 (group 2) as vulnerable-mildly frail, patients who scored 8–9 (group 3) as severely frail.

2.6. Routine laboratory biomarkers

Complete blood count with differential, and serum concentrations C-reactive protein (CRP), D-dimer, sodium, potassium, procalcitonin, were measured by standard procedures. Serum IL-6 was determined by using the high-sensitivity ProQuantum qPCR immunoassay (Thermo Fisher) measured on the Aria Mix real-time PCR system (Agilent) following the manufacturer's protocol. Each sample was assayed in duplicate. GFR was estimated according to Chronic Kidney Disease Epidemiology Collaboration (CKD-EPI) equation (Levey et al., 2009).

2.7. Small RNA sequencing analysis (NGS) of 12 COVID-19 plasma samples

Plasma RNA samples of 12 COVID-19 patients were subjected to small-RNA sequencing. TruSeq Small RNA Library PrepKit v2 (Illumina; RS-200–0012/24/36/48) was used for library preparation according to the manufacturer's indications. Briefly, 35 ng purified RNA was linked to RNA 3' and 5' adapters, converted to cDNA, and amplified using Illumina primers containing unique indexes for each sample. Each library was quantified using Agilent Bioanalyzer and High Sensitivity DNA Kit (cat. no. 5067–4626, Agilent Technologies, USA), and equal amounts of libraries were pooled together. Size selection allowed keeping 130–160 bp fragments. After ethanol precipitation, the library pool was quantified with Agilent High Sensitivity DNA Kit, diluted to 1.8 pM, and sequenced using NextSeq® 500/550 High Output Kit v2 (75 cycles) (Illumina; FC-404-2005) on the Illumina NextSeq500 platform.

Raw base-call data generated by the Illumina NextSeq 500 system were demultiplexed using Illumina BaseSpace Sequence Hub (https://basespace.illumina.com/home/index) and converted to FASTQ format. After a quality check with FastQC (https://www.bioinformatics.babraham.ac.uk/projects/fastqc/), the adapter sequences were trimmed using Cutadapt (Martin, 2011), which also removed sequences < 10 nucleotides. Reads were mapped using the STAR algorithm (Dobin et al., 2012). The reference genome consisted of human miRNA sequences from the miRbase 21 database (Kozomara et al., 2019). Raw counts from mapped reads were obtained using the htseq-count script from the HTSeq tools (Anders et al., 2014). Raw counts were further normalized using the DESeq2 Bioconductor package (Love et al., 2014).

Raw and processed datasets have been deposited in NCBI's Gene Expression Omnibus (GEO) (https://www.ncbi.nlm.nih.gov/geo) with accession reference GSE189506.

2.8. Quantitative real-time polymerase chain reaction

MiRNAs differentially expressed in the setting of COVID-19 patients analyzed in the discovery phase were then validated by qRT-PCR in the validation phase analyzing a cohort of 116 COVID-19 patients. In the validation phase, selected miRNAs were reverse transcribed using the TaqMan miRNA Reverse Transcription Kit (Life Technologies, Carlsbad, CA, United States) as recommended by the manufacturer and quantified by a miRNA assay (Applied Biosystems, Foster City, CA, USA).

Relative quantification was performed using the $2^{-\Delta Cq}$ method (ΔCq = CqmicroRNA-Cqcel-miR-39-3p). Synthetic cel-miR-39-3p was spiked-in before RNA isolation for normalization in subsequent qRT-PCR. Based on the lowest coefficient of variation (CV) from the small RNA-seq, we selected two miRNAs, i.e., miR-92a and miR-103, which were used for the calculation of the RE through the $2^{-\Delta Ct}$ normalization method. The spike-in cell-miR-39 was also used for normalization. The three miRNAs chosen for normalization were also combined using the geometric mean of the relative quantities (i.e., 2^{-Ct}[miRNA]) to obtain a normalization factor. Relative expression (RE) of each miRNA was therefore reported as the ratio between miRNA relative quantity on the normalization factor (D'Haene et al., 2012), and expressed as arbitrary units.

2.9. Pathway analysis of miRNA targets

The resultant miRNAs were analyzed through the use of IPA (Ingenuity Pathway Analysis, QIAGEN, Germany) to explore the experimentally observed High Predicted and Moderate Predicted mRNA Targets (Supplementary Table 1) via the microRNA Target Filter Analysis. Targets were predicted using the TargetScan algorithm by searching for the presence of conserved 8mer and 7mer sites that match the seed region of each microRNA. Experimentally demonstrated microRNA/mRNA were identified using content from TarBase with miRBase identifiers. Experimentally validated human, rat, and mouse microRNA-mRNA interactions were identified from ~550 published articles and Ingenuity® Knowledge Base (thousands of microRNA-related findings manually curated from published literature by Ingenuity scientific experts).

2.10. Statistical analysis

NGS data were analyzed using Genespring GX software v14.8 (Agilent Technologies). The miRNAs showing a differential expression were identified by comparing patients alive or deceased during the in-hospital stay, using a fold change ≥ 1.5 filter and FDR 5% at moderated *t*-test with Benjamini-Hochberg correction. Cluster analysis was performed using GeneSpring GX software with Manhattan correlation as a similarity measure.

Continuous variables, including miRNA serum levels, were reported as either mean and standard deviation or median and interquartile range based on their distribution (assessed using the Shapiro-Wilk test). MiRNA expression levels were also dichotomized based on the upper quintile as the cut-off point. Comparison of variables between groups was performed by unpaired Student t-test or Mann-Whitney U test as appropriate. The association between miRNA levels and in-hospital death was investigated by Kaplan Meier curves, log-rank test for equality of survivor functions, and by Cox proportional hazards analysis (age- and gender-adjusted and age-, gender- and IL-6 adjusted hazard ratios (HR) and 95% confidence intervals (95% CI).

A two-tailed P value < 0.05 was considered significant. Data were analyzed using STATA version15.1 Statistical Software Package for Windows (Stata Corp, College Station, TX).

3. Results

Table 1a summarizes the main demographic and biochemical characteristics of the discovery cohort, which includes 12 COVID-19 patients, 6 survived and 6 deceased during in-hospital stay for COVID-19. None of the analyzed parameters was significantly different between survived and deceased patients. Median time from symptom onset to hospital admission was comparable between the two groups. However,

through the small RNA-seq analysis, we identified 34 serum miRNAs significantly modulated between survived and deceased patients at the time of hospital admission (Table 2 and Fig. 1). Among the 34 differentially expressed miRNAs, 25 were down-regulated and 9 were up-regulated in deceased compared to survived COVID-19 patients (Table 2 and Fig. 1). Among miRNAs detected in all samples by the small RNA-seq, those with the lowest CV, i.e., miR-92a-3p (17.4%) and miR-103a-3p (20.8%) were chosen as internal controls for the validation phase, in addition to the exogenous spike-in cel-miR-39.

MiRNAs showing the highest modulation and the highest expression levels were considered as suitable candidates for the validation phase of the study. Specifically, we selected i) the most differentially regulated miRNAs with a qPCR probe available for our detection system, i.e., miR-339-3p (down) and miR-483-5p (up), and ii) the differentially regulated miRNAs with the highest mean of normalized counts, i.e., miR-146a-5p, miR-106b-5p, miR-222-3p, miR-221-3p, and miR-320b. Therefore, a final panel including seven miRNAs was analyzed through qRT-PCR in serum samples from the validation cohort of 116 COVID-19 patients. MiR-339-3p and miR-222-3p were excluded from the subsequent analyses because their validation yielded high Ct values (>33) in all samples tested, suggesting their negligible expression (data not shown).

The main demographic, biochemical, and clinical characteristics of the validation cohort are described in Table 1b. Deceased patients were significantly older than survivors, and showed significantly increased levels of creatinine, eGFR, CRP, procalcitonin, IL-6, total white blood cells (WBC), neutrophil, lymphocyte, monocyte, eosinophil count, and neutrophil/lymphocyte ratio (NLR). Regarding the comorbidities, increased prevalence of atrial fibrillation, chronic obstructive pulmonary disease (COPD), and CKD was observed among deceased patients

Table 1a
Baseline demographical and biochemical characteristics of survived and deceased COVID-19 patients of the discovery cohort.

Variables	Total (n = 12)	Survived (n = 6)	Deceased (n = 6)	p-value
Age (years)	75.4 (5.9)	74.7 (3.0)	76.2 (8.2)	0.682
Gender (Males, %)	6 (50%)	3 (50%)	3 (50%)	–
Median time between onset of symptoms to hospital admission (days)	7.0 [0.0–14.0]	7.0 [1.8–12.3]	7.5 [1.3–13.0]	1.000
Glucose (mg/dL)	115 (26)	109 (9)	122 (36)	0.396
Creatinine (mg/dL)	1.17 (0.85)	0.90 (0.43)	1.44 (1.10)	0.291
eGFR (mL/min)	74 (18)	83 (15)	66 (19)	0.224
CRP (mg/dL)	10.4 (7.4)	8.4 (5.9)	12.5 (8.6)	0.354
Pro-calcitonin (ng/mL)	0.33 (0.54)	0.09 (0.09)	0.56 (0.70)	0.135
IL-6 (pg/mL)	124.2 (267.6)	18.4 (14.2)	229.9 (361.2)	0.211
Hemoglobin (g/dL)	11.9 (2.3)	12.6 (1.2)	11.3 (3.0)	0.369
Platelets (n/mm^3)	189 (58)	209 (56)	169 (57)	0.254
WBC ($\times10^3$/mm^3)	5.70 (2.76)	6.06 (3.11)	5.34 (2.60)	0.676
Neutrophils ($\times10^3$/mm^3)	4.73 (2.73)	4.96 (3.11)	4.50 (2.57)	0.788
Lymphocytes ($\times10^3$/mm^3)	0.62 (0.33)	0.71 (0.32)	0.53 (0.33)	0.372
Monocytes ($\times10^3$/mm^3)	0.32 (0.14)	0.34 (0.17)	0.30 (0.13)	0.626
Eosinophils ($\times10^3$/mm^3)	0.03 (0.03)	0.04 (0.04)	0.01 (0.01)	0.232
Basophils ($\times10^3$/mm^3)	0.01 (0.01)	0.02 (0.02)	0.01 (0.01)	0.363
NLR	9.5 (6.4)	8.4 (6.3)	10.5 (6.7)	0.593
D-dimer (ng/mL)	1185 (1467)	1795 (1945)	575 (237)	0.186
NLR	9.48 (6.41)	8.42 (6.26)	10.54 (6.97)	0.593
dNLR	5.52 (3.41)	4.99 (3.19)	6.05 (3.84)	0.616
PLR	378.9 (230.4)	335.7 (119.1)	422.0 (313.2)	0.550
LMR	2.31 (1.41)	2.58 (1.63)	2.03 (1.23)	0.526

Data are mean (SD) and median [IQR]. P value from t-test for continuous variables and from chi-squared tests of association for categorical variables. CRP, C-reactive protein; eGFR, estimated glomerular filtration rate; NLR, neutrophil-to-lymphocyte ratio; dNLR, derived NLR; PLR, platelet-to-lymphocyte ratio; LMR, lymphocyte-to-monocyte ratio; WBC, white blood cells.

Table 1b
Comparison of biochemical and anthropometric characteristics between survived and deceased COVID-19 patients of the validation cohort.

Variables	Total (n = 116)	Survived (n = 75)	Deceased (n = 41)	p-value
Age (years)	86.5 (82–91)	84 (81–90)	90 (85–93)	**< 0.001**
Gender (Males, %)	39 (33.6%)	25 (33.3%)	14 (34.2%)	0.929
Median time between onset of symptoms to hospital admission (days)	8.0 (3.5–13.0)	8.0 (2.0–13.0)	9.0 (4.0–13.0)	0.995
CFS, n (%)				**0.005**
0–3	18 (15.5%)	16 (21.3%)	2 (4.9%)	
4–7	58 (50.0%)	40 (53.3%)	18 (43.9%)	
8–9	38 (32.8%)	17 (22.7%)	21 (51.2%)	
NA	2 (1.7%)	2 (2.7%)	0 (0.0%)	
Glucose (mg/dL)	108 (89–134)	106 (89–133)	112.5 (91–163)	0.574
Creatinine (mg/dL)	0.8 (0.6–1.2)	0.8 (0.6–1.1)	1.0 (0.8–1.9)	**0.002**
eGFR (mL/min)	72 (49–85)	80 (56–88)	53 (30–79)	**< 0.001**
CRP (mg/dL)	3.5 (1.3–8.7)	2.3 (0.8–6.1)	9.2 (2.4–13.1)	**< 0.001**
Pro-calcitonin (ng/mL)	0.05 (0.05–0.25)	0.05 (0.05–0.15)	0.18 (0.08–0.94)	**< 0.001**
IL-6 (pg/mL)	73.2 (36.1–156.9)	50.6 (26.9–139.2)	99.0 (54.9–239.2)	**0.002**
Hemoglobin (g/dL)	11.6 (10.2–13.1)	11.7 (10.2–13.1)	11.6 (9.9–12.8)	0.761
Platelets (n/mm^3)	233 (177–300)	252 (182–311)	215 (123–264)	0.060
WBC ($\times10^3$/mm^3)	8.5 (5.4–11.8)	7.9 (4.9–10.1)	11.8 (7.1–16.0)	**0.001**
Neutrophils ($\times10^3$/mm^3)	6.0 (4.3–9.3)	5.5 (4.2–7.6)	8.3 (5.7–13.8)	**0.021**
Lymphocytes ($\times10^3$/mm^3)	1.11 (0.78–1.65)	1.22 (0.84–1.65)	0.91 (0.49–1.62)	**0.029**
Monocytes ($\times10^3$/mm^3)	0.47 (0.32–0.64)	0.50 (0.36–0.65)	0.39 (0.24–0.53)	**0.017**
Eosinophils ($\times10^3$/mm^3)	0.01 (0–0.06)	0.02 (0–0.06)	0 (0–0.02)	**0.001**
Basophils ($\times10^3$/mm^3)	0.01 (0.01–0.02)	0.01 (0.01–0.02)	0.01 (0.01–0.02)	0.311
D-dimer (ng/mL)	1090 (750–2010)	1090 (750–1950)	1245 (700–4075)	0.537
NLR	5.22 (3.18–9.33)	4.40 (2.71–7.79)	8.93 (5.22–17.51)	**< 0.001**
dNLR	2.03 (0.77–4.11)	2.00 (0.89–3.39)	3.11 (0.42–6.06)	0.256
PLR	208.0 (134.2–328.8)	202.3 (134.2–291.1)	246.5 (127.4–384.4)	0.353
LMR	2.38 (1.60–3.64)	2.43 (1.75–3.64)	2.11 (1.23–3.67)	0.526
Comorbidities, n (%)				
Hypertension	75 (66.4%)	48 (65.8%)	27 (67.5%)	0.851
Type 2 Diabetes	27 (23.9%)	21 (28.8%)	6 (15%)	0.101
Stroke	15 (13.3%)	7 (9.6%)	8 (20%)	0.119
Cancer	23 (20.4%)	18 (24.7%)	5 (12.5%)	0.125
COPD	17 (15%)	7 (9.6%)	10 (25%)	**0.028**
Asthma	3 (2.7%)	3 (4.1%)	0 (0%)	0.194
Angina	1 (0.9%)	1 (1.4%)	0 (0%)	0.457
Myocardial infarction	14 (12.4%)	8 (11%)	6 (15%)	0.533
AF	33 (29.2%)	16 (21.9%)	17 (42.5%)	**0.021**
Heart failure	34 (30.1%)	18 (24.7%)	16 (40%)	0.089
AD	9 (8%)	4 (5.5%)	5 (12.5%)	0.187
Non-AD dementia	34 (30.1%)	21 (28.8%)	13 (32.5%)	0.679
CKD	26 (23%)	12 (16.4%)	14 (35%)	**0.025**
Treatments				
Glucocorticoids, n (%)	98 (84.5%)	64 (85.3%)	34(82.9%)	0.732
Heparin, n (%)	106 (91.4%)	67 (89.3%)	39 (95.1%)	0.288

Data are median (IQR). P value from *t*-test for continuous variables and from chi-squared tests of association for categorical variables. CFS, Clinical Frailty Scale; AF, Atrial fibrillation; AD, Alzheimer's disease; CKD, chronic kidney disease; COPD, chronic obstructive pulmonary disease. NLR, neutrophil-to-lymphocyte ratio; dNLR, derived NLR; PLR, platelet-to-lymphocyte ratio; LMR, lymphocyte-to-monocyte ratio; WBC, white blood cells.

compared to the survivors. The analysis of the Clinical Frailty Scale (CSF) revealed that the percentage of severely frail patients was increased in deceased patients (51.2%), compared to the survived ones (22.7%).

Table 3 summarizes the serum expression values of the five selected miRNAs analyzed in the validation cohort. Two of the five selected miRNAs, i.e., miR-320b and miR-483-5p, were significantly upregulated at the time of hospital admission in deceased patients compared to survived ones. The serum expression levels of these two miRNAs, obtained both using miR-92a levels for normalization and combining the relative quantities of three miRNAs, i.e., cel-miR-39, miR-103, and miR-92a for normalization, were more than two-fold higher in deceased patients compared to survived ones (Table 3 and Fig. 2).

No significant associations were observed between serum miRNA levels and fasting glucose, CRP, and IL-6 (data not shown). Significant negative correlations were observed between miR-320b serum levels and eosinophil count (Table 4 and Supplementary Table 1).

Kaplan-Meier analysis for the estimation of survival over time confirmed that mortality was significantly higher in patients with the highest serum miR-320b levels (upper quintile as a cut-off point), using both the geometric mean of internal controls ($p = 0.008$; Fig. 3A) and miR-103a ($p = 0.003$; data not shown) as normalizers, while no difference was observed for miR-483–5p ($p = 0.067$; Fig. 3B).

Cox regression analysis, adjusted for age and gender (model 1), confirmed that miR-320b (RE to miR-92a and RE to miR-103a) and miR-483-5p serum levels (independently from normalization), as continuous variables, were significantly associated with an increased risk of in-hospital mortality (Table 5 and Supplementary Table 2). When the expression levels were dichotomized based on the upper quintile as the cut-off point, Cox regression model 1 confirmed that patients with the highest miR-320b levels (expressed both as RE to CN and RE to miR-103a) showed a 2-fold increased risk of death compared to patients with lower miR-320b serum level.

Further models, adjusted for relevant confounders (in addition to age and gender), including IL-6 and CSF (model 2), and IL-6, CSF, CKD, COPD, and atrial fibrillation (model 3), confirmed that patients having serum miR-320b levels (expressed both as RE to CN and RE to miR-103a) in the upper quintile showed 2-fold increased risk of death compared to patients with lower serum miR-320b (Table 5).

All the mRNA targets of miR-320b and miR-483-5p, experimentally observed and highly or moderately predicted, identified by Ingenuity Pathway Analysis (IPA) software, were listed in Supplementary Table 3. These targets belong to several pathways, including Acute Phase Response Signaling and Airway Pathology in Chronic Obstructive Pulmonary Disease. Supplementary Figure 1 depicts the highly and moderately predicted targets of both miR-320b and miR-483–5p and highlights four common mRNA targets.

4. Discussion

The stratification of COVID-19 patients based on the risk of developing the most severe outcomes currently remains extremely challenging for physicians. In this framework, the availability of innovative, minimally invasive biomarkers with prognostic relevance could help to identify, especially among older comorbid patients, those at higher risk of developing severe COVID-19. We conducted a two-phase study, including discovery and validation phases, for identifying circulating serum miRNAs associated with COVID-19 in-hospital mortality, by analyzing two independent samples of patients, enrolled in two different hospitals of Ancona, Italy. Through a small RNA-seq analysis of 12 serum samples collected for the discovery phase, we identified 34 miRNAs significantly modulated in deceased compared to survived

Table 2
MicroRNA significantly associated with in-hospital mortality in the discovery cohort.

MiRNA annotation	Mean of normalized mean count	Sum of normalized read counts	Moderated T-Test, p*	Modulation	|Fold change| (D vs S)
hsa-miR-8061	5.3	63.2	0.002	down	27.17
hsa-miR-339-3p	12.8	153.9	0.028	down	15.08
hsa-miR-181c-3p	2.0	24.3	0.003	down	14.42
hsa-miR-146a-5p	21.7	260.5	**0.070**	**down**	**13.20**
hsa-miR-582-3p	5.2	62.8	0.062	down	9.92
hsa-miR-17-p	9.8	117.8	0.048	down	9.65
hsa-miR-101-5p	1.6	19.6	0.025	down	8.93
hsa-miR-941	4.5	53.7	0.083	down	8.78
hsa-miR-410-3p	1.1	13.3	0.009	down	8.46
hsa-miR-422a	2.7	32.6	0.057	down	8.46
hsa-miR-551a	7.2	85.9	0.079	down	8.16
hsa-miR-106b-5p	16.2	194.3	**0.080**	**down**	**7.69**
hsa-miR-222-3p	17.4	208.9	0.083	down	7.69
hsa-miR-424-5p	2.1	24.7	0.069	down	7.64
hsa-miR-185-3p	2.5	30.3	0.088	down	6.89
hsa-miR-342-3p	3.0	35.7	0.093	down	6.79
hsa-miR-361-5p	1.9	22.6	0.087	down	6.52
hsa-miR-28-5p	1.1	13.4	0.043	down	6.37
hsa-miR-411-5p	1.4	16.4	0.066	down	5.54
hsa-miR-152-3p	0.7	8.5	0.051	down	5.00
hsa-miR-1843	0.6	7.7	0.057	down	4.38
hsa-miR-18a-5p	0.5	6.5	0.051	down	4.35
hsa-miR-542-3p	0.6	7.3	0.075	down	3.82
hsa-miR-18b-5p	0.5	5.6	0.061	down	3.74
hsa-miR-378f	0.3	3.9	0.062	down	3.28
hsa-miR-1285-5p	6.5	78.2	0.016	up	19.97
hsa-miR-483-5p	4.5	53.8	**0.069**	**up**	**7.93**
hsa-miR-328-3p	5.0	59.9	0.079	up	7.56
hsa-miR-378c	51.8	621.9	0.060	up	7.23
hsa-miR-203a-3p	0.6	7.6	0.046	up	5.02
hsa-miR-34a-5p	0.9	10.8	0.074	up	4.90
hsa-miR-100-5p	40.5	485.5	0.047	up	4.58
hsa-miR-221-3p	243.6	2923.6	**0.044**	**up**	**2.60**
hsa-miR-320b	366.3	4395.9	**0.092**	**up**	**3.80**

* corrected p-value cut-off: 0.1. Fold change>= 2.0, D vs S. D, deceased patients; S, survived patients. In italic miRNAs validated in the validation cohort; in bold italic miRNAs detectable in the validation phase (Ct<33) and considered for the survival analyses.

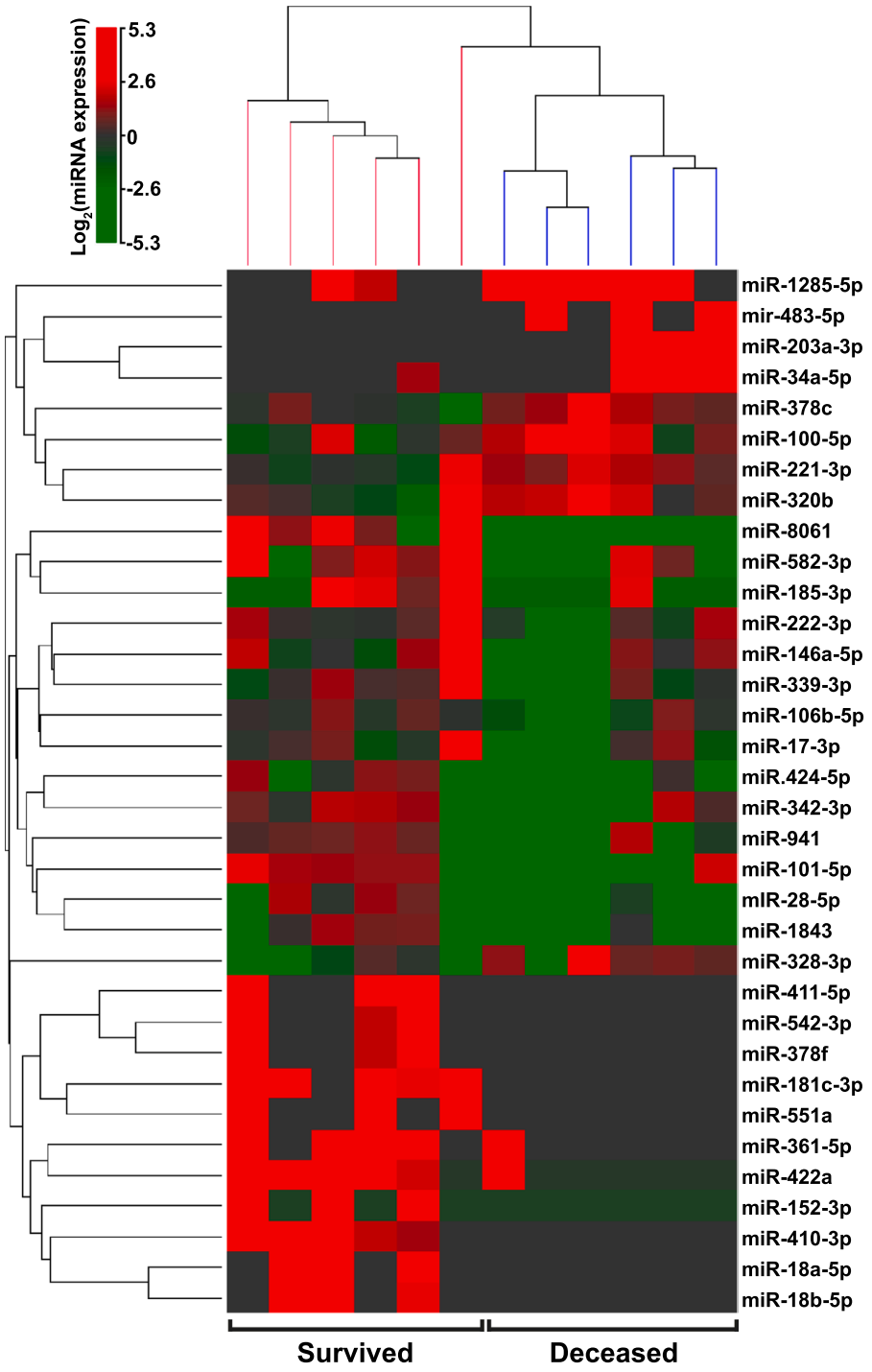

Fig. 1. Hierarchical Combined Tree of microRNAs analyzed in discovery cohort. MiRNAs showing a FC $\geq$ 2.0 and p $<$ 0.1 at moderated *t*-test between deceased and survived patients are represented. The heatmap diagrams show the centered miRNA expression values in logarithmic scale across the groups of samples.

patients during the in-hospital stay. By selecting miRNAs with the highest modulation and expression levels, we identified 5 miRNAs for the subsequent validation in 116 COVID-19 serum samples. MiR-320b and miR-483–5p were identified as significantly upregulated miRNAs at the time of admission in deceased patients compared to survived ones, suggesting a potential prognostic relevance if assessed at hospital admission. Few studies until now have explored circulating miRNAs as diagnostic and prognostic tools in COVID-19 (Farr et al., 2021; Paul et al., 2022). MiR-320 family, including miR-320a, miR-320b, and miR-320c, was recently associated with COVID-19 severity (Duecker et al., 2021). The pathway analysis of Kyoto encyclopedia of genes and genomes (KEGG) revealed their involvement in the transforming growth factor (TGF)-β signaling pathway and in the regulation of adherens junctions, suggesting that miR-320 family members could be related to pro-inflammatory and thromboembolic processes observed in patients with respiratory failure (Duecker et al., 2021). We observed significant negative correlations between miR-320b serum levels and eosinophil count. Recently, miR-320b expression was demonstrated to be different between eosinophils from asthmatics and healthy subjects (Rodrigo-Munoz et al., 2019). Further, the upregulation of miR-320b was previously observed in the failing heart of patients with diabetes mellitus and in a well-established mouse model for diabetes mellitus and diabetic

Table 3
MicroRNAs significantly associated with in-hospital mortality in the validation cohort.

MiRNAs	Total (N = 116)	Survived (N = 75)	Dead (N = 41)	p (Mann-Whitney)
RE to combined normalizer				
miR-106b-5p	0.098 (0.070–0.158)	0.096 (0.067–0.154)	0.102 (0.074–0.162)	0.736
miR-146a-5p	0.081 (0.046–0.125)	0.076 (0.053–0.117)	0.086 (0.040–0.149)	0.718
miR-221–3p	0.062 (0.032–0.106)	0.070 (0.034–0.108)	0.055 (0.032–0.106)	0.612
miR-320b	0.140 (0.086–0.311)	0.120 (0.077–0.245)	0.195 (0.112–0.463)	**0.013**
miR-483–5p	0.061 (0.020–0.174)	0.043 (0.017–0.123)	0.094 (0.024–0.252)	**0.035**
RE to cel-miR-39				
miR-106b-5p	0.004 (0.002–0.008)	0.004 (0.002–0.008)	0.003 (0.001–0.007)	0.432
miR-146a-5p	0.003 (0.001–0.006)	0.003 (0.002–0.006)	0.003 (0.001–0.006)	0.605
miR-221–3p	0.002 (0.001–0.005)	0.003 (0.001–0.005)	0.002 (0.001–0.004)	0.479
miR-320b	0.005 (0.003–0.012)	0.004 (0.002–0.011)	0.008 (0.003–0.021)	0.062
miR-483–5p	0.002 (0.001–0.007)	0.002 (0.001–0.006)	0.003 (0.001–0.009)	0.079
RE to miR-92a				
miR-106b-5p	0.073 (0.039–0.132)	0.073 (0.042–0.120)	0.072 (0.037–0.132)	0.993
miR-146a-5p	0.057 (0.028–0.099)	0.051 (0.028–0.092)	0.062 (0.027–0.108)	0.599
miR-221–3p	0.040 (0.020–0.090)	0.045 (0.021–0.094)	0.038 (0.019–0.078)	0.593
miR-320b	0.101 (0.051–0.215)	0.079 (0.041–0.193)	0.156 (0.071–0.219)	**0.033**
miR-483-5p	0.035 (0.013–0.137)	0.026 (0.012–0.089)	0.083 (0.014–0.268)	**0.033**
RE to miR-103				
miR-106b-5p	3.618 (2.505–5.657)	3.593 (2.667–5.408)	3.978 (2.145–5.918)	0.946
miR-146a-5p	2.761 (1.879–4.675)	2.667 (1.790–4.438)	2.849 (2.049–5.420)	0.541
miR-221–3p	2.173 (1.248–3.732)	2.282 (1.329–3.399)	2.129 (1.181–3.784)	0.960
miR-320b	5.187 (2.949–11.876)	4.724 (2.928–9.221)	7.235 (3.458–21.259)	0.062
miR-483–5p	1.906 (0.678–5.579)	1.662 (0.705–4.757)	4.584 (0.653–13.682)	0.054

RE, relative expression. Common normalizer is the geometric mean of (2-Ct [normalizer]). In bold miRNAs differentially expressed between survived and deceased patients.

complications that lead to heart failure (Li et al., 2019). Unexpectedly, in the same study it was demonstrated that miR-320 acts as a small activating RNA in the nucleus at the level of transcription (Li et al., 2019). Several evidence suggested that miR-320 can contribute to glucose and lipid metabolism via different signaling pathways. Indeed, nuclear miR-320 could mediate diabetes-induced cardiac dysfunction by activating the transcription of fatty acid metabolic genes to cause lipotoxicity in the heart (Du et al., 2021). It was also reported that miR-320 exerts an anti-angiogenic function in type 2 diabetic rats (Wang et al., 2014), and negatively regulates the expression of VEGF, the main transcription factor for endothelial cells, through ERK 1/2 (Feng and Chakrabarti, 2012).

Interestingly, low miR-320b expression levels were associated with reduced survival of COPD patients (Keller et al., 2019). Albeit COPD and severe COVID-19 pneumonia share some clinicopathological features, the former condition arises from long-lasting chronic airway inflammation, while the latter is characterized by a variety of extrapulmonary features, including an acute systemic immune response (Ramos-Casals et al., 2021). Thus, it is conceivable that these differences could be reflected also by circulating miRNAs. In our study, we observed a significantly higher prevalence of COPD in COVID-19 deceased patients (25%) compared to survived ones (9.6%). Therefore, we cannot exclude the possibility that the expression levels of miR-320b in the validation cohort of COVID-19 patients could be influenced by the presence of COPD.

We could hypothesize that the increased circulating miR-320b levels could mark eosinophil dysfunction, endothelial dysfunction, and lipotoxicity in the heart, all features that may be associated with the spreading of SARS-CoV-2 infection.

Two mature miRNAs, i.e., miR-483-5p and miR-483-3p, originate from the *MIR483* gene, which is located within the insulin-like growth factor 2 (IGF2) locus. This gene shows an independent expression from its host gene *IGF2*, even if in *IGF2* producing non-islet cell tumor hypoglycemia (NICTH), miR-483 family is suggested to be co-expressed with IGF-2 (Nagao et al., 2021). The miR-483 family affects glucose metabolism, as well as the Wnt/β-catenin, TGF-β, and TP53 signaling pathways by targeting several genes, including *IGF1* (Pepe et al., 2018). Overexpressing miR-483–3p in diabetic transgenic mice was sufficient to exacerbate cardiomyocyte apoptosis by transcriptionally repressing *IGF1*, suggesting a signaling pathway involving miR-483-3p-IGF1 in the promotion of myocardial cell apoptosis under high blood-glucose conditions (Qiao et al., 2016). MiR-483-5p was identified as a relevant target in the prevention of cardiometabolic disease (Gallo et al., 2021).

Overall, glucose/lipidic metabolism and *IGF1* gene expression seem to be targeted by both miR-320b and miR-483-3p/5p (Du et al., 2021; Zhou et al., 2021), and both miRNAs are responsive to short-term intensive insulin therapy (IIT) (Nunez Lopez et al., 2019).

Recently, circulating miR-483-3p expression levels were analyzed in children affected by severe pneumonia demonstrating that patients with high expression of miR-483–3p had higher mortality (Zhou et al., 2021). Overexpression of miR-483–3p was associated with the suppression of cell proliferation and the production of inflammatory cytokines (Zhou et al., 2021). To this regard, miR-483–5p upregulation in the lung tissues of sepsis-induced acute lung injury (ALI) mice suggested a correlation between infection and the up-regulation of this miRNA (Leng et al., 2020). Knockdown of miR-483–5p effectively ameliorated lung injury in mice with sepsis-induced ALI and inhibited inflammation and apoptosis of LPS-treated cellular models (Leng et al., 2020).

Notably, a recent genome-wide serum miRNA expression profile in chronic kidney disease (CKD) patients identified miR-483–5p as potential diagnostic biomarkers for CKD (Liu et al., 2020). In our study, we observed an increased prevalence of CKD in COVID-19 deceased patients (35%) compared to survived ones (16%). Notably, microRNA profiling of atrial tissue biopsies showed that miR-483–5p is the most upregulated miRNA in patients who developed postoperative atrial fibrillation after coronary artery bypass grafting (Harling et al., 2017). Moreover, a 16-year follow-up study revealed that circulating miR-483–5p predicts the onset of type 2 diabetes and cardiovascular disease, including myocardial infarction (Gallo et al., 2018), suggesting that this miRNA could be secreted from the heart in conditions of cardiac wall stress. We cannot exclude the possibility that the increased expression levels of miR-483–5p in COVID-19 patients with the most severe outcome could be related, at least in part, to the presence of CKD and/or atrial fibrillation.

Regarding serum levels of miR-146a that we previously identified as significantly associated with the response to anti-IL-6 receptor drug Tocilizumab (Sabbatinelli et al., 2021), we did not observe significant differences between survived and deceased patients in the validation cohort. This group of patients was not treated with Tocilizumab, suggesting that miR-146a serum levels could be related to anti-IL-6 receptor treatment efficacy rather than to COVID-19 mortality.

Finally, technical challenges exist in measuring extracellular miRNA,

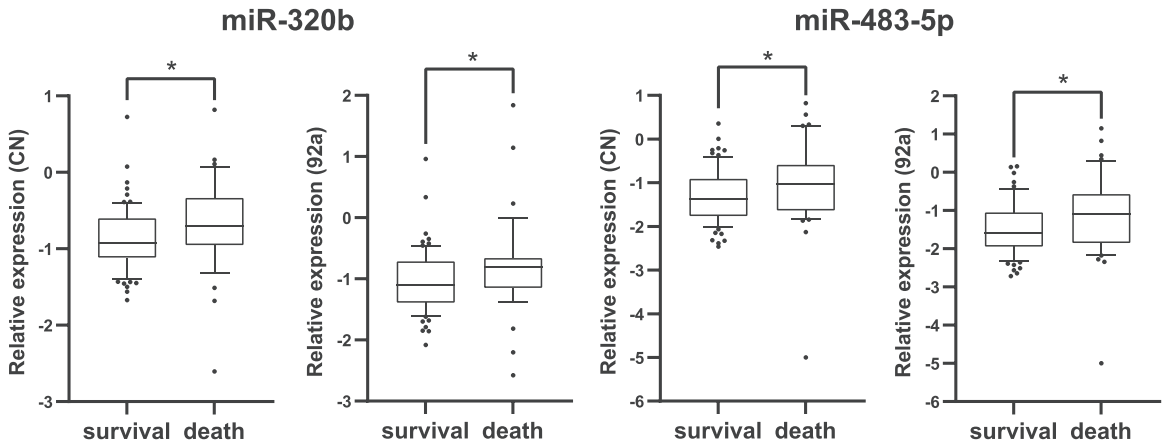

Fig. 2. MiR-320b (RE to CN and RE to miR-92a) and miR-483-5p (RE to CN and RE to miR-92a) in survived and deceased COVID-19 patients of the validation cohort. MiR-320b (RE to CN and RE to miR-92a) and miR-483–5p (RE to CN and RE to miR-92a). RE CN = relative expression normalized by the geometric mean of (2-Ct [normalizer]). * , $p < 0.05$.

Table 4
Correlation coefficients of serum microRNAs with absolute (n) and percentage (%) counts of WBC populations.

MiRNAs	Basophils		Eosinophils		Lymphocytes		Neutrophils	
	Abs. count	%	Abs. count	%	Abs. count	%	Abs. count	%
RE to combined normalizer								
miR-106b-5p	0.0174	-0.0592	-0.035	-0.0221	-0.0611	0.0602	-0.0729	0.038
miR-146a-5p	0.1914	0.1922	0.005	0.0697	0.0421	0.1834	0.055	-0.0389
miR-221-3p	0.198	0.0807	0.1801	0.0754	0.0313	-0.0589	0.0891	0.1583
miR-320b	-0.0781	-0.1996	**-0.3097***	-0.206	-0.2124	-0.1401	0.0741	0.1238
miR-483-5p	-0.0498	-0.1419	-0.0921	-0.2038	-0.0824	-0.0814	-0.0206	0.144
RE to miR-92a								
miR-106b-5p	0.063	0.0829	0.0892	0.1534	-0.0712	0.0514	-0.1108	0.036
miR-146a-5p	0.1441	**0.2759***	0.1072	0.1681	0.0587	0.1864	-0.0838	-0.0574
miR-221-3p	0.1737	0.1736	0.1951	0.1049	0.0378	-0.0246	0.0219	0.1442
miR-320b	0.0353	-0.0278	**-0.2257***	-0.1117	-0.2089	-0.1456	0.1029	0.1523
miR-483-5p	-0.0219	-0.0277	-0.0688	-0.1707	-0.109	-0.0534	-0.045	0.1448

RE, relative expression. Common normalizer is the geometric mean of (2-Ct[normalizer]).

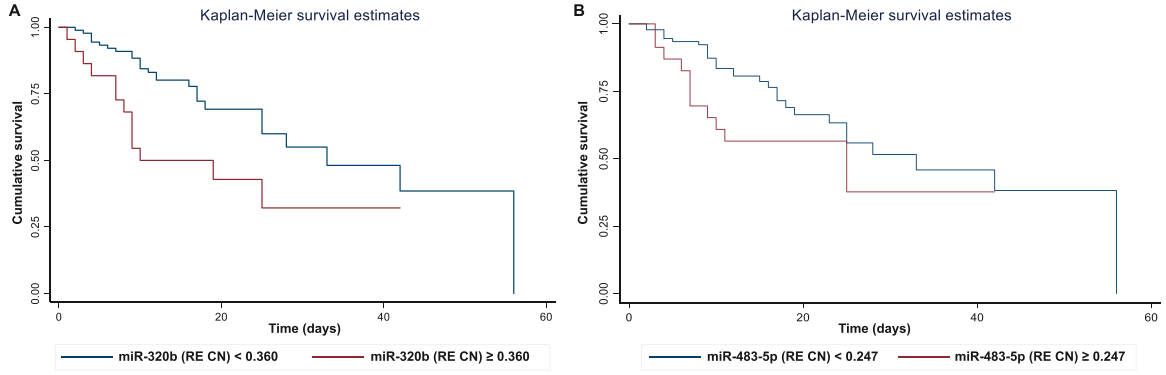

Fig. 3. Kaplan-Meier survival function for patients in the validation cohort stratified according to (A) miR-320b (upper quintile, RE ≥ 0.360 vs. lowest quintiles, RE < 0.360) and (B) miR-483–5p (upper quintile, RE ≥ 0.247 vs. lowest quintiles, RE < 0.247) serum levels. RE CN = relative expression normalized by the geometric mean of (2^{-Ct}[normalizer]).

especially in normalization methods. Because of the relatively low expression of miRNAs in serum/plasma, conventional methods of spectrophotometry are not reliable to control for the total amount of RNA extracted from different samples. Here, we used different strategies for miRNA normalization, including the geometric mean of three different normalizers, two selected from the small RNA-seq analysis, and the spike in miRNA cel-miR-39, as previously described (D'Haene et al., 2012). We observed that miRNA normalized as relative to the geometric mean of three different normalizers showed better performances in the statistical analysis.

Overall, higher circulating levels of miR-320b and miR-483–5p assessed at the time of admission are significantly associated with an increased risk of COVID-19 in-hospital mortality. We suggest that their measurement at hospital admission could help to stratify COVID-19 patients based on mortality risk, especially concerning the oldest COVID-19 patients.

Table 5
Cox regression analysis of survival on the validation cohort.

	Model 1: Age and gender		Model 2: Model 1 + IL-6 and CSF	Model 3: Model 2 + COPD, CKD, and AF
MiRNAs	Continuous	Dichotomous (cut-off: upper 20%)	Dichotomous (cut-off: upper 20%)	Dichotomous (cut-off: upper 20%)
	HR (95%CI)	HR (95%CI)	HR (95%CI)	HR (95%CI)
miR-320b RE to CN	1.20 (0.90–1.59)	**2.31 (1.18–4.55)**	**2.75 (1.36–5.53)**	**2.88 (1.26–6.57)**
miR-320b RE to miR-92a	**1.11 (1.02–1.22)**	1.44 (0.68–3.06)	1.74 (0.80–3.76)	2.20 (0.86–5.64)
miR-483–5p RE to CN	**1.41 (1.10–1.82)**	1.86 (0.92–3.75)	**2.63 (1.24–5.57)**	**3.99 (1.72–9.26)**
miR-483–5p RE to miR-92a	**1.21 (1.07–1.38)**	1.53 (0.75–3.12)	1.55 (0.76–3.16)	1.79 (0.79–4.07)

RE, relative expression; CN, common normalizer. CN is the geometric mean of (2-Ct[normalizer]). CFS, Clinical Frailty Scale; CKD, chronic kidney disease; COPD, chronic obstructive pulmonary disease; AF: atrial fibrillation. In bold miRNAs with statistical associations with mortality.

Sources of funding

This work was supported by the Italian Ministry of Health, Italy, (Ricerca Corrente to IRCCS INRCA) and by Università Politecnica delle Marche ,Italy, (RSA grant to FO and ADP).

Conflict of Interest

The authors declare that they have no conflict of interest.

Data availability

Raw and processed datasets of the small RNA-seq of the discovery cohort have been deposited in NCBI's Gene Expression Omnibus (GEO) (https://www.ncbi.nlm.nih.gov/geo) with accession reference GSE189506.

Appendix A. Supporting information

Supplementary data associated with this article can be found in the online version at doi:10.1016/j.mad.2022.111636.

References

Ahmad, F., Kannan, M., Ansari, A.W., 2021. Role of SARS-CoV-2 -induced cytokines and growth factors in coagulopathy and thromboembolism. Cytokine Growth Factor Rev.
Anders, S., Pyl, P.T., Huber, W., 2014. HTSeq—a Python framework to work with high-throughput sequencing data. Bioinformatics 31, 166–169.
Bonafè, M., Prattichizzo, F., Giuliani, A., Storci, G., Sabbatinelli, J., Olivieri, F., 2020. Inflamm-aging: Why older men are the most susceptible to SARS-CoV-2 complicated outcomes. Cytokine Growth Factor Rev. 53, 33–37.
Campochiaro, C., Tomelleri, A., Matucci-Cerinic, M., Dagna, L., 2021. One year later: the case of tocilizumab in COVID-19. Eur. J. Intern. Med.
Cavalli, G., Larcher, A., Tomelleri, A., Campochiaro, C., Della-Torre, E., De Luca, G., Farina, N., Boffini, N., Ruggeri, A., Poli, A., Scarpellini, P., Rovere-Querini, P., Tresoldi, M., Salonia, A., Montorsi, F., Landoni, G., Castagna, A., Ciceri, F., Zangrillo, A., Dagna, L., 2021. Interleukin-1 and interleukin-6 inhibition compared with standard management in patients with COVID-19 and hyperinflammation: a cohort study. Lancet Rheumatol. 3, e253–e261.
Charlson, M.E., Pompei, P., Ales, K.L., MacKenzie, C.R., 1987. A new method of classifying prognostic comorbidity in longitudinal studies: development and validation. J. Chronic Dis. 40, 373–383.
Chen, Y.M., Zheng, Y.L., Su, X., Wang, X.Q., 2021. Crosstalk between MicroRNAs and circular RNAs in human diseases: a bibliographic study. Front. Cell Dev. Biol. 9, 754880.
D'Haene, B., Mestdagh, P., Hellemans, J., Vandesompele, J., 2012. miRNA expression profiling: from reference genes to global mean normalization. Methods Mol. Biol. 822, 261–272.
de Gonzalo-Calvo, D., Benitez, I.D., Pinilla, L., Carratala, A., Moncusi-Moix, A., Gort-Paniello, C., Molinero, M., Gonzalez, J., Torres, G., Bernal, M., Pico, S., Almansa, R., Jorge, N., Ortega, A., Bustamante-Munguira, E., Gomez, J.M., Gonzalez-Rivera, M., Micheloud, D., Ryan, P., Martinez, A., Tamayo, L., Aldecoa, C., Ferrer, R., Ceccato, A., Fernandez-Barat, L., Motos, A., Riera, J., Menendez, R., Garcia-Gasulla, D., Penuelas, O., Torres, A., Bermejo-Martin, J.F., Barbe, F., Project, C., 2021. Circulating microRNA profiles predict the severity of COVID-19 in hospitalized patients. Transl. Res. 236, 147–159.
Della-Torre, E., Lanzillotta, M., Campochiaro, C., Cavalli, G., De Luca, G., Tomelleri, A., Boffini, N., De Lorenzo, R., Ruggeri, A., Rovere-Querini, P., Castagna, A., Landoni, G., Tresoldi, M., Ciceri, F., Zangrillo, A., Dagna, L., 2021. Respiratory impairment predicts response to IL-1 and IL-6 blockade in COVID-19 patients with severe pneumonia and hyper-inflammation. Front. Immunol. 12, 675678.
Dobin, A., Davis, C.A., Schlesinger, F., Drenkow, J., Zaleski, C., Jha, S., Batut, P., Chaisson, M., Gingeras, T.R., 2012. STAR: ultrafast universal RNA-seq aligner. Bioinformatics 15–21.
Du, H., Zhao, Y., Yin, Z., Wang, D.W., Chen, C., 2021. The role of miR-320 in glucose and lipid metabolism disorder-associated diseases. Int. J. Biol. Sci. 17, 402–416.
Duecker, R.P., Adam, E.H., Wirtz, S., Gronau, L., Khodamoradi, Y., Eberhardt, F.J., Donath, H., Gutmann, D., Vehreschild, M., Zacharowski, K., Kreyenberg, H., Chiocchetti, A.G., Zielen, S., Schubert, R., 2021. The MiR-320 family is strongly downregulated in patients with COVID-19 induced severe respiratory failure. Int. J. Mol. Sci. 22.
Elezkurtaj, S., Greuel, S., Ihlow, J., Michaelis, E.G., Bischoff, P., Kunze, C.A., Sinn, B.V., Gerhold, M., Hauptmann, K., Ingold-Heppner, B., Miller, F., Herbst, H., Corman, V. M., Martin, H., Radbruch, H., Heppner, F.L., Horst, D., 2021. Causes of death and comorbidities in hospitalized patients with COVID-19. Sci. Rep. 11, 4263.
Farr, R.J., Rootes, C.L., Rowntree, L.C., Nguyen, T.H.O., Hensen, L., Kedzierski, L., Cheng, A.C., Kedzierska, K., Au, G.G., Marsh, G.A., Vasan, S.S., Foo, C.H., Cowled, C., Stewart, C.R., 2021. Altered microRNA expression in COVID-19 patients enables identification of SARS-CoV-2 infection. PLoS Pathog. 17, e1009759.
Feng, B., Chakrabarti, S., 2012. miR-320 regulates glucose-induced gene expression in diabetes. ISRN Endocrinol. 2012, 549875.
Gallo, W., Esguerra, J.L.S., Eliasson, L., Melander, O., 2018. miR-483-5p associates with obesity and insulin resistance and independently associates with new onset diabetes mellitus and cardiovascular disease. PLoS One 13, e0206974.
Gallo, W., Ottosson, F., Kennback, C., Jujic, A., Esguerra, J.L.S., Eliasson, L., Melander, O., 2021. Replication study reveals miR-483-5p as an important target in prevention of cardiometabolic disease. BMC Cardiovasc. Disord. 21, 162.
Group, W.H.O.R.E.A.f.C-T.W., Shankar-Hari, M., Vale, C.L., Godolphin, P.J., Fisher, D., Higgins, J.P.T., Spiga, F., Savovic, J., Tierney, J., Baron, G., Benbenishty, J.S., Berry, L.R., Broman, N., Cavalcanti, A.B., Colman, R., De Buyser, S.L., Derde, L.P.G., Domingo, P., Omar, S.F., Fernandez-Cruz, A., Feuth, T., Garcia, F., Garcia-Vicuna, R., Gonzalez-Alvaro, I., Gordon, A.C., Haynes, R., Hermine, O., Horby, P.W., Horick, N. K., Kumar, K., Lambrecht, B.N., Landray, M.J., Leal, L., Lederer, D.J., Lorenzi, E., Mariette, X., Merchante, N., Misnan, N.A., Mohan, S.V., Nivens, M.C., Oksi, J., Perez-Molina, J.A., Pizov, R., Porcher, R., Postma, S., Rajasuriar, R., Ramanan, A.V., Ravaud, P., Reid, P.D., Rutgers, A., Sancho-Lopez, A., Seto, T.B., Sivapalasingam, S., Soin, A.S., Staplin, N., Stone, J.H., Strohbehn, G.W., Sunden-Cullberg, J., Torre-Cisneros, J., Tsai, L.W., van Hoogstraten, H., van Meerten, T., Veiga, V.C., Westerweel, P.E., Murthy, S., Diaz, J.V., Marshall, J.C., Sterne, J.A.C., 2021. Association between administration of IL-6 antagonists and mortality among patients hospitalized for COVID-19: a meta-analysis. J. Am. Med. Assoc. 499–518.
Gutmann, C., Khamina, K., Theofilatos, K., Diendorfer, A.B., Burnap, S.A., Nabeebaccus, A., Fish, M., McPhail, M.J.W., O'Gallagher, K., Schmidt, L.E., Cassel, C., Auzinger, G., Napoli, S., Mujib, S.F., Trovato, F., Sanderson, B., Merrick, B., Roy, R., Edgeworth, J.D., Shah, A.M., Hayday, A.C., Traby, L., Hackl, M., Eichinger, S., Shankar-Hari, M., Mayr, M., 2021. Association of cardiometabolic microRNAs with COVID-19 severity and mortality. Cardiovasc. Res.
Harling, L., Lambert, J., Ashrafian, H., Darzi, A., Gooderham, N.J., Athanasiou, T., 2017. Elevated serum microRNA 483-5p levels may predict patients at risk of post-operative atrial fibrillation. Eur. J. Cardiothorac. Surg. 51, 73–78.
Jia, F., Wang, G., Xu, J., Long, J., Deng, F., Jiang, W., 2021. Role of tumor necrosis factor -alpha in the mortality of hospitalized patients with severe and critical COVID-19 pneumonia. Aging 13.
Keller, A., Ludwig, N., Fehlmann, T., Kahraman, M., Backes, C., Kern, F., Vogelmeier, C. F., Diener, C., Fischer, U., Biertz, F., Herr, C., Jorres, R.A., Lenhof, H.P., Bals, R., Meese, E., 2019. Low miR-150-5p and miR-320b expression predicts reduced survival of COPD patients. Cells 8.
Kozomara, A., Birgaoanu, M., Griffiths-Jones, S., 2019. miRBase: from microRNA sequences to function. Nucleic Acids Res. 47, D155–D162.
Leng, C., Sun, J., Xin, K., Ge, J., Liu, P., Feng, X., 2020. High expression of miR-483-5p aggravates sepsis-induced acute lung injury. J. Toxicol. Sci. 45, 77–86.

Levey, A.S., Stevens, L.A., Schmid, C.H., Zhang, Y.L., Castro 3rd, A.F., Feldman, H.I., Kusek, J.W., Eggers, P., Van Lente, F., Greene, T., Coresh, J., Ckd, E.P.I., 2009. A new equation to estimate glomerular filtration rate. Ann. Intern. Med. 150, 604–612.

Li, H., Fan, J., Zhao, Y., Zhang, X., Dai, B., Zhan, J., Yin, Z., Nie, X., Fu, X.D., Chen, C., Wang, D.W., 2019. Nuclear miR-320 mediates diabetes-induced cardiac dysfunction by activating transcription of fatty acid metabolic genes to cause lipotoxicity in the heart. Circ. Res. 125, 1106–1120.

Liu, T., Feng, M., Wen, Z., He, Y., Lin, W., Zhang, M., 2021. Comparison of the characteristics of cytokine storm and immune response induced by SARS-CoV, MERS-CoV, and SARS-CoV-2 infections. J. Inflamm. Res. 14, 5475–5487.

Liu, X., Wang, W., Bai, Y., Zhang, H., Zhang, S., He, L., Zhou, W., Zhang, D., Xu, J., 2020. Identification of a genome-wide serum microRNA expression profile as potential noninvasive biomarkers for chronic kidney disease using next-generation sequencing. J. Int. Med. Res. 48, 300060520969481.

Lo, C.K.L., Chagla, Z., 2021. In patients hospitalized for COVID-19, tocilizumab reduces mortality at 28 d. Ann. Intern. Med. 174, JC125.

Love, M.I., Huber, W., Anders, S., 2014. Moderated estimation of fold change and dispersion for RNA-seq data with DESeq2. Genome Biol. 15, 550.

Malgie, J., Schoones, J.W., Zeegers, M.P., Pijls, B.G., 2021. Decreased mortality and increased side effects in COVID-19 patients treated with IL-6 receptor antagonists: systematic review and meta-analysis. Sci. Rep. 11, 21522.

Martin, M., 2011. Cutadapt removes adapter sequences from high-throughput sequencing reads. 2011 17, 3.

Mehta, P., McAuley, D.F., Brown, M., Sanchez, E., Tattersall, R.S., Manson, J.J., Hlh Across Speciality Collaboration, U.K, 2020. COVID-19: consider cytokine storm syndromes and immunosuppression. Lancet 395, 1033–1034.

Nagao, M., Fukuda, I., Asai, A., Esguerra, J.L.S., Hizuka, N., Eliasson, L., Sugihara, H., 2021. Diagnostic potential of miR-483 family for IGF-II producing non-islet cell tumor hypoglycemia. Eur. J. Endocrinol. 184, 41–49.

Nunez Lopez, Y.O., Retnakaran, R., Zinman, B., Pratley, R.E., Seyhan, A.A., 2019. Predicting and understanding the response to short-term intensive insulin therapy in people with early type 2 diabetes. Mol. Metab. 20, 63–78.

Olivieri, F., Prattichizzo, F., Giuliani, A., Matacchione, G., Rippo, M.R., Sabbatinelli, J., Bonafe, M., 2021. miR-21 and miR-146a: The microRNAs of inflammaging and age-related diseases. Ageing Res. Rev. 70, 101374.

Olivieri, F., Rippo, M.R., Procopio, A.D., Fazioli, F., 2013. Circulating inflamma-miRs in aging and age-related diseases. Front. Genet. 4, 121.

Parray, A., Mir, F.A., Doudin, A., Iskandarani, A., Danjuma, M.M., Kuni, R.A.T., Abdelmajid, A., Abdelhafez, I., Arif, R., Mulhim, M., Abukhattab, M., Dar, S.R., Moustafa, A.A., Elkord, E., Al Khal, A.L., Elzouki, A.N., Cyprian, F., 2021. SnoRNAs and miRNAs networks underlying COVID-19 disease severity. Vaccines 9.

Paul, S., Bravo Vazquez, L.A., Reyes-Perez, P.R., Estrada-Meza, C., Aponte Alburquerque, R.A., Pathak, S., Banerjee, A., Bandyopadhyay, A., Chakraborty, S., Srivastava, A., 2022. The role of microRNAs in solving COVID-19 puzzle from infection to therapeutics: a mini-review. Virus Res. 308, 198631.

Pepe, F., Visone, R., Veronese, A., 2018. The glucose-regulated MiR-483-3p influences key signaling pathways in cancer. Cancers 10.

Pomponio, G., Ferrarini, A., Bonifazi, M., Moretti, M., Salvi, A., Giacometti, A., Tavio, M., Titolo, G., Morbidoni, L., Frausini, G., Onesta, M., Amico, D., Rocchi, M.L.B., Menzo, S., Zuccatosta, L., Mei, F., Menditto, V., Svegliati, S., Donati, A., D'Errico, M. M., Pavani, M., Gabrielli, A., 2021. Tocilizumab in COVID-19 interstitial pneumonia. J. Intern. Med. 289, 738–746.

Qiao, Y., Zhao, Y., Liu, Y., Ma, N., Wang, C., Zou, J., Liu, Z., Zhou, Z., Han, D., He, J., Sun, Q., Liu, Y., Xu, C., Du, Z., Huang, H., 2016. miR-483-3p regulates hyperglycaemia-induced cardiomyocyte apoptosis in transgenic mice. Biochem. Biophys. Res. Commun. 477, 541–547.

Ramos-Casals, M., Brito-Zeron, P., Mariette, X., 2021. Systemic and organ-specific immune-related manifestations of COVID-19. Nat. Rev. Rheumatol. 17, 315–332.

Rockwood, K., Song, X., MacKnight, C., Bergman, H., Hogan, D.B., McDowell, I., Mitnitski, A., 2005. A global clinical measure of fitness and frailty in elderly people. CMAJ 173, 489–495.

Rodrigo-Munoz, J.M., Canas, J.A., Sastre, B., Rego, N., Greif, G., Rial, M., Minguez, P., Mahillo-Fernandez, I., Fernandez-Nieto, M., Mora, I., Barranco, P., Quirce, S., Sastre, J., Del Pozo, V., 2019. Asthma diagnosis using integrated analysis of eosinophil microRNAs. Allergy 74, 507–517.

Ruan, Q., Yang, K., Wang, W., Jiang, L., Song, J., 2020. Correction to: Clinical predictors of mortality due to COVID-19 based on an analysis of data of 150 patients from Wuhan, China. Intensive Care Med. 46, 1294–1297.

Sabbatinelli, J., Giuliani, A., Matacchione, G., Latini, S., Laprovitera, N., Pomponio, G., Ferrarini, A., Svegliati Baroni, S., Pavani, M., Moretti, M., Gabrielli, A., Procopio, A. D., Ferracin, M., Bonafè, M., Olivieri, F., 2021. Decreased serum levels of the inflammaging marker miR-146a are associated with clinical non-response to tocilizumab in COVID-19 patients. Mech. Ageing Dev. 193, 111413.

Vela, D., Vela-Gaxha, Z., Rexhepi, M., Olloni, R., Hyseni, V., Nallbani, R., 2021. Efficacy and safety of tocilizumab versus standard care/placebo in patients with COVID-19; a systematic review and meta-analysis of randomized clinical trials. Br. J. Clin. Pharmacol.

Wang, X., Huang, W., Liu, G., Cai, W., Millard, R.W., Wang, Y., Chang, J., Peng, T., Fan, G.C., 2014. Cardiomyocytes mediate anti-angiogenesis in type 2 diabetic rats through the exosomal transfer of miR-320 into endothelial cells. J. Mol. Cell Cardiol. 74, 139–150.

Wu, C., Chen, X., Cai, Y., Xia, J., Zhou, X., Xu, S., Huang, H., Zhang, L., Zhou, X., Du, C., Zhang, Y., Song, J., Wang, S., Chao, Y., Yang, Z., Xu, J., Zhou, X., Chen, D., Xiong, W., Xu, L., Zhou, F., Jiang, J., Bai, C., Zheng, J., Song, Y., 2020. Risk factors associated with acute respiratory distress syndrome and death in patients with coronavirus disease 2019 pneumonia in Wuhan, China. JAMA Intern. Med. 180, 934–943.

Zhou, J., Lin, J., Zhao, Y., Sun, X., 2021. Deregulated expression of miR-483-3p serves as a diagnostic biomarker in severe pneumonia children with respiratory failure and its predictive value for the clinical outcome of patients. Mol. Biotechnol.

Zhou, P., Yang, X.L., Wang, X.G., Hu, B., Zhang, L., Zhang, W., Si, H.R., Zhu, Y., Li, B., Huang, C.L., Chen, H.D., Chen, J., Luo, Y., Guo, H., Jiang, R.D., Liu, M.Q., Chen, Y., Shen, X.R., Wang, X., Zheng, X.S., Zhao, K., Chen, Q.J., Deng, F., Liu, L.L., Yan, B., Zhan, F.X., Wang, Y.Y., Xiao, G.F., Shi, Z.L., 2020. A pneumonia outbreak associated with a new coronavirus of probable bat origin. Nature 579, 270–273.